Part-regularized Near-duplicate Vehicle Re-identification

Bing He[1] Jia Li[1,3,4*] Yifan Zhao[1] Yonghong Tian[2,3]

[1]State Key Laboratory of Virtual Reality Technology and Systems, SCSE, Beihang University
[2]National Engineering Laboratory for Video Technology, School of EE&CS, Peking University
[3]Peng Cheng Laboratory, Shenzhen, China
[4]Beijing Advanced Innovation Center for Big Data and Brain Computing, Beijing, China

[1]{bing, jiali, zhaoyf}@buaa.edu.cn [2]yhtian@pku.edu.cn

Abstract

Vehicle re-identification (Re-ID) has been attracting more interests in computer vision owing to its great contributions in urban surveillance and intelligent transportation. With the development of deep learning approaches, vehicle Re-ID still faces a near-duplicate challenge, which is to distinguish different instances with nearly identical appearances. Previous methods simply rely on the global visual features to handle this problem. In this paper, we proposed a simple but efficient part-regularized discriminative feature preserving method which enhances the perceptive ability of subtle discrepancies. We further develop a novel framework to integrate part constrains with the global Re-ID modules by introducing an detection branch. Our framework is trained end-to-end with combined local and global constrains. Specially, without the part-regularized local constrains in inference step, our Re-ID network outperforms the state-of-the-art method by a large margin on large benchmark datasets VehicleID and VeRi-776.

1. Introduction

Given a query image of a vehicle identity, vehicle re-identification task aims to retrieve all the images of this identity from a large image database which typically captured from a large camera network. With the proposals of large dataset [14, 12, 27]and the development of deep learning algorithms [24, 36], recent models have gain remarkable success in the past decade. The re-identification of vehicles has a great potential to contribute to the urban security surveillance and intelligent transportation.

Considering the inconspicuous divergences among different instances, vehicle re-identification is still a very challenging task, especially with the large amount of dataset. To address this Re-ID task, many deep learning models [27, 1] relied on global information have been proposed in the past decades. One intuitive solution is to reduce the distances of identical vehicle images and enlarge the distance of different ones with learning approaches. To better measure the distance, previous works [12] mainly use deep metric learning to directly embed the raw image into an Euclidean space where the distance can be directly used as similarity scores between two vehicles. Weinberger *et al.* [25] explore the topic of metric learning to perform k-nearest neighbor classification and propose the Large Margin Nearest Neighbor loss (LMNN). FaceNet [20] improved the LMNN loss into a modified triplet loss which directly optimize the final distance metric and can be applied in re-identification and face recognition tasks. Although these works reach remarkable success in vehicle re-identification tasks, they usually get confused when these vehicle have inconspicuous differences. *e.g.*, see Fig. 1 (a).

(a) (b)

Figure 1. Near-duplicate problem. (a) Images in each row all come from different vehicle identities with similar appearance. Apparently it is difficult to distinguish them especially the first row since all three vehicle identities come from a same vehicle model. Subtle discriminative vehicle parts are crucial for the near-duplicate vehicle re-identification. (b) As shown in the right side of the image those similar vehicles are easy to distinguish using the local part feature.

*Jia Li is the corresponding author. URL: http://cvteam.net

To handle this problem, recent works resort to additional license plate and spatial-temporal information. Liu *et al.* [14] introduce license plate recognition into Re-ID task. The license plate recognition usually fails in unconstrained environment due to the various viewpoints and changeable illuminations. However, owing to the privacy and security considerations in vehicle re-identification task, the plate information is inaccessible in the public benchmarks. Besides, Some other methods [21, 24] rely on extra spatial-temporal information to explore the final retrieval results.

In this paper, we explore the near-duplicate phenomenon in vehicle re-identification. As illustrated in Fig. 1 a), different vehicles usually share similar geometric shapes and appearances which can be hard to distinguish by deep models. While the details from these near-duplicate vehicles have arresting variances in local features such as brands and tags in windows which are easily recognized by human beings, see Fig. 1 b). To handle the near duplicated phenomenon in vehicle re-identification task, we propose a part-regularized approach which integrates the local and no-local features into a unified architecture. To avoid the vanish of local features, we enhance the perception of local information of regularized parts in deep learning networks. Inspired by ROI (region of interest) in object detection, we adopt ROI receptive module to capture the local information. We develop a simple but effective ROI projection approach to combine detection branch with our Re-ID task. After combining these features, we further developed a local and no-local classification loss. To summarize, the contribution of our work is three-fold:

- We design an effective representation learning framework by jointly considering local and global representations.
- We propose a part-regularized approach to enhance the discriminative capability of global features for vehicle re-identification.
- We conduct extensive experiments to show that the proposed approach outperforms state-of-the-art: VehicleID [12] by 57% in rank-1, 23% in rank-5, VeRi-776 [14] by 48% in mAP, 2.1% in HIT@1 and 9.6% in HIT@5.

The rest of this paper is organized as follows: Sec. 2 reviews the related works, Sec. 3 gives the problem statement of vehicle re-identification and explains the details of our part-regularized model. Qualitative and quantitative experiments are presented in Sec. 4 and we finally conclude our paper in Sec. 5.

2. Related Work

Vehicle Re-ID. The vehicle re-identification task has gained more and more attention in recent years. Liu *et al.* [12] proposed a benchmark dataset VehicleID and a pipeline which use Deep Relative Distance Learning (DRDL) to project vehicle images into an Euclidean space, where the distance can directly measure the similarity of two vehicle images. Liu *et al.* [14]proposed another dataset, which called VeRi-776, and build a coarse-to-fine progressive search framework through utilizing the visual appearance, license plate and spatial-temporal information. VeRi-776 contains rich annotations including vehicle types, colors, brands, license plate and spatio-temporal information. Wang *et al.* [24] explored vehicle viewpoint attribute and proposed orientation invariant feature embedding module. The orientations information are extracted by 20 vehicle key points locations. Shen *et al.* [21] pushed spatial-temporal idea further and proposed Visual-spatial-temporal Path Proposals method. Yan *et al.* [27] model the relationships of vehicle images as multi-grain list and proposes two ranking methods, generalized pairwise ranking and multi-grain based list ranking to address this problem, and contributed two high-quality and well-annotated vehicle datasets VD1 and VD2, which are collected from two different cities with diverse annotated attributes. While Lou *et al.* [15] resort to adversarial learning to generate cross views of new examples.

Person Re-ID. Person re-identification aims to retrieve all the images of the query individual from a large scale image database. The person re-id methods can be roughly categorized into two groups, classification methods and Siamese methods based on triplet comparisons. Li *et al.* [7] proposed a multi-scale context aware network that can capture knowledge of the local context. Xiao *et al.* [26] proposed a model to learn deep feature representations from multiple dataset with Convolutional Neural Networks.Their experiment shows that some neurons learn representations shared across all datasets, while some others are effective only for a specific domain. Su *et al.* [22] proposed a pose-driven convolutional neural network to address the large pose deformations and the complex view variations problem. AlignedReID [31] learns a global feature but performs part alignment during training. local feature is extracted by horizontal pooling from each row, without requiring additional supervision or pose estimation.

Discriminative part localization. Discriminative part localization has been studied for a long time by many community such as fine-grained recognition [5, 10, 18, 29, 30], face recognition [37, 16, 17, 33, 23] and person re-identification [26]. After deep learning dominate computer vision community, hand-craft part features for fine-grained recognition has been drooped. Many works [34, 8] in person re-identification exploited human body parts to learn robust representations. Li *et al.* [8] proposed to learn and localize deformable pedestrian parts using Spatial Transformer Networks(STN). Using semantic segmentation' s a-

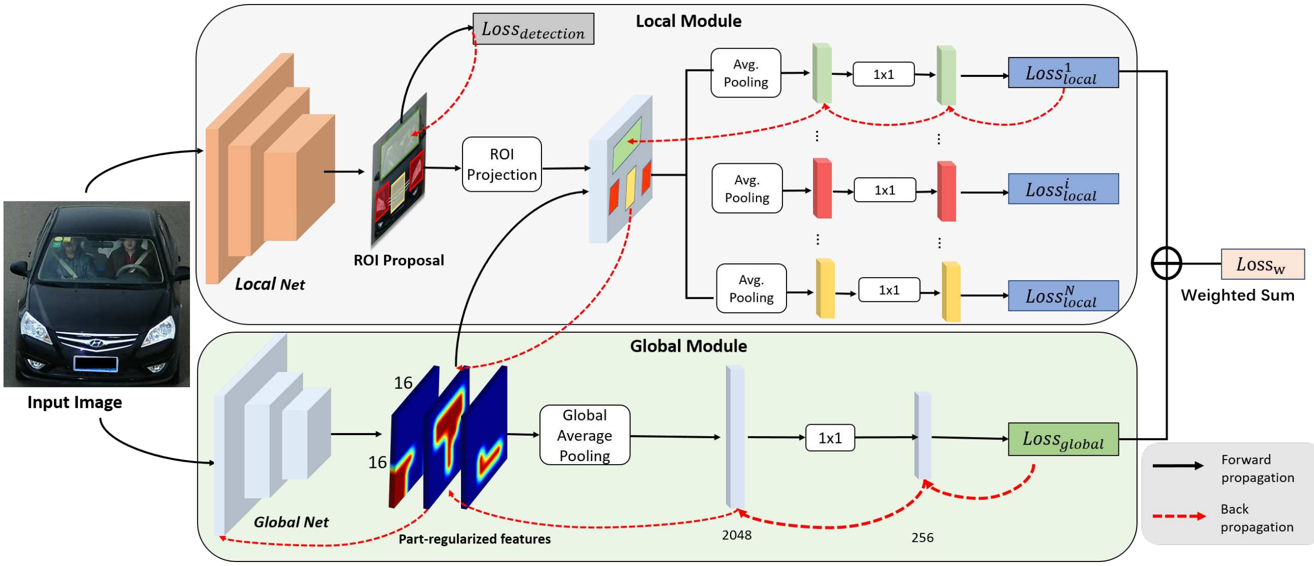

Figure 2. The pipeline of our framework. Our framework consist of two modules, a local module which focuses on the part features to distinguish the subtle discrepancy in visual features and a global module which is regularized by the part attentions in the local module. A part-localization network and a new objective is introduced to encourage correct classification of the identified parts. The LocalNet is a common object detection network which generates the ROI of each vehicle part. After that, in every local part branch, we project the ROIs generated by the part localization module into the global feature map. Specially, we only use the global module (in green) to conduct our inference which is already regularized by the part features in back propagation process.

bility of localizing the various human part precisely under severe pose variations, Kalayeh *et al.* [6] exploited human semantic parsing to harness local visual cues for vehicle re-identification. Fu *et al.* [3] proposed a weakly supervised recurrent attention convolutional neural network to recursively learn discriminative region attention and region-based feature representation. Picking deep filter responses [32] proposed to learn part detectors in an unsupervised way by analyzing filter response from deep convolutional neural network.

3. Methodology

3.1. Problem Statement

Given a query image, the target of vehicle re-identification is to compute the similarity score between this query image and all the other images in the gallery. Define the training set as $\{x_i, y_i\}_{i=1}^{N}$. Each vehicle image x_i is labeled with identification label y_i with the total number of N training images. The training Images and identification labels are denoted as $\boldsymbol{x}$ and $\boldsymbol{y}$ respectively. The desired similarity between probe p and gallery image g is defined as $M(\phi(p;\boldsymbol{\theta}), \phi(g;\boldsymbol{\theta}))$, where $\phi(\cdot;\boldsymbol{\theta})$ is the feature extraction function which usually denotes a common deep encoder, and $M(\cdot)$ is a metric defined in the feature space. The most important question is how to learn the feature extraction function $\phi(\cdot;\boldsymbol{\theta})$. Previous works use classification method to learn parameters $\boldsymbol{\theta}$ in function $\phi(\cdot;\boldsymbol{\theta})$, from which the optimization target can be defined as

$$\arg\min_{\boldsymbol{\theta}} \mathbb{E}\left(\phi(\boldsymbol{x};\boldsymbol{\theta})^{\top}\boldsymbol{w}, \boldsymbol{y}\right), \quad (1)$$

where $\phi(\boldsymbol{x};\boldsymbol{\theta})$is the feature extracted by deep neural network with parameter $\boldsymbol{\theta}$, $\boldsymbol{w}$ is the parameter to project the features into predicted labels. $\mathbb{E}(\cdot)$ is the cross entropy loss. As discussed before, the equations above only optimize the global feature and become easy to ignore subtle visual cues. To handle this problem, We introduce part information and propose a novel local feature based optimization target which is defined as

$$\arg\min_{\boldsymbol{\theta}} \mathbb{E}\left(\phi(\boldsymbol{x};\boldsymbol{\theta})^{\top}\boldsymbol{w}_g, \boldsymbol{y}\right) + \sum_{p\in\mathbb{P}} \lambda_p \mathbb{E}\left(\left(\phi(\boldsymbol{x};\boldsymbol{\theta}) \circledast M_p\right)^{\top} \boldsymbol{w}_l, \boldsymbol{y}_p\right), \quad (2)$$

where $\boldsymbol{w}_g$ is the parameter to project the global feature into predicted identification label. $\boldsymbol{w}_l$ is the local parameter that project the local part feature into predicted part label. M_p is the part location that can be used to extract local feature from global feature. $\circledast$ is the local feature extraction operation. This formulation introduce the part constrain to the re-id task and force the network preserve the local part cue to recognize parts. Details will be explained in section 3.2.

There are still some unsolved problems in Eq. (2). First, the part set $\mathbb{P}$ is not defined which means we don't know which part should be used. Second, The part location M_p need to be extracted. Third, $\boldsymbol{y}_p$, which is the part label, should be determined. In the next subsection, we will explain our network structure to address these problems.

3.2. Part-Regularized Re-ID

In this section, we introduce part regularized (PR) constrains into the vehicle re-identification task. Our framework consists of two components, a global module to conduct Re-ID categorization and a local part-regularized module to encourage correct classification of the identified parts. To preserve better context information, which is very crucial for the near-duplicate problem, we adopt bounding box detection network for part localization. We will explain the details of the two main components in this section and describe training scheme in section 3.3.

Part definition. We select three vehicle parts for our part detection module, lights, including front light and back light, window, including front window and back window, and vehicle brand. The vehicle head area is crucial to distinguish different vehicle model. we use the front lights to inference the vehicle head area including the brand. Different model may have extremely diffidence lights, we define bounding box of the light as tight bounding box contains the light but extend it to the bottom of the vehicle. This definition can preserve more context information which we find more stable in experiment. The definition of the three parts in our model is shown in Fig. 3. We draw N local branches in Fig. 2 since our framework is flexible to various definitions of vehicle parts, and we only test N = 3 parts (window, light, brand) to validate the effectiveness of this framework.

Part detection. To solve the second problem, we need to find the parts location of the training images. There are many off the shelf object part localization algorithms, which can mainly categorize into two classes, detection and segmentation. Segmentation method need pixel level annotation which is difficult to get. In this paper we use a detection branch to detect the predefined vehicle parts. As shown in the Fig. 2, raw vehicle image is fed into the $LocalNet$ (use YOLO in experiments), which has 24 convolutional layers, to get raw part detection results. A desired result is that every image get three bounding box for window, left light and right light respectively. During the training process, we find that in some rare cases the vehicle part detection model may fail due to occlusion. To handle these invisible parts in a specific vehicle image, we refer to the rest images of the same vehicle and compute the average locations of the missing parts. After that, these average part locations are used as the pseudo detection results of this specific image to facilitate the subsequent training process.

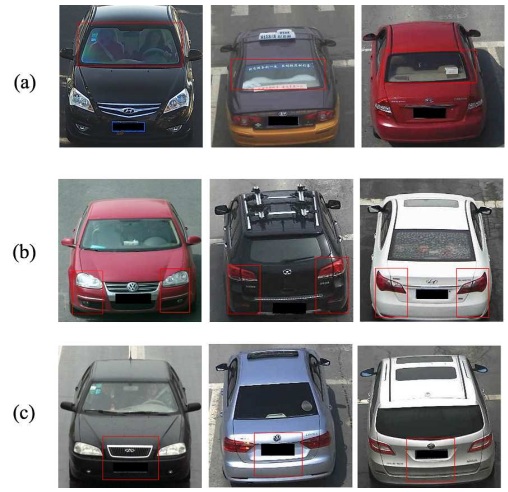

Figure 3. The part definition of our model. The first row shows the vehicle window part in both front and back view. Vehicle lights are shown in the second row. We extend the bounding box of the lights to the bottom of the vehicle to preserve more context information. The head and rear area of the vehicle containing the vehicle brand is defined as vehicle brand part.

Part-based Feature Extraction and Aggregation. Our part-based feature extraction and aggregation module has one global branch and three local part branch. All four branches share the same backbone network, any convolutional backbone can be used here, we use ResNet-50 [4] in this paper. All input image were re-sized into $H \times W$ to generate feature map with shape $S \times S \times C$. The global branch simply use global average pooling to generate the global feature vector. In every local part branch, we project the ROI generated by the part localization module into the global feature map. We divided the input image into an $S \times S$ grid where $S \times S$ equals the spatial size of the global feature map($S \times S$). Every grid cell overlapped with the ROI would be marked as that part corresponding to the ROI. After that local part feature vector will be extracted use local average pooling.

Now we have part set $\mathbb{P}$ and part localization M_p in Eq. (2), we need to define the part label $\boldsymbol{y}_p$ to train the network. However part label is very difficult to obtained. For example, the brand part label may be set as the name of vehicle manufacturer, since all the brand from the same manufacturer should be same. The window part, on the other hand, contains personalize cue of a specific vehicle, so it should labeled with that specific vehicle identity. Considering vehicle model and vehicle make information is not available in some scenario, we propose to use vehicle identification label to approximate the part label, Eq. (2) can be

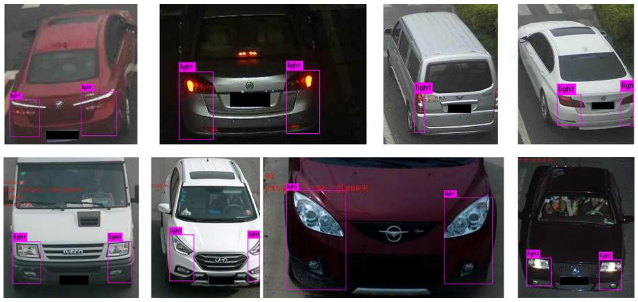

(a)

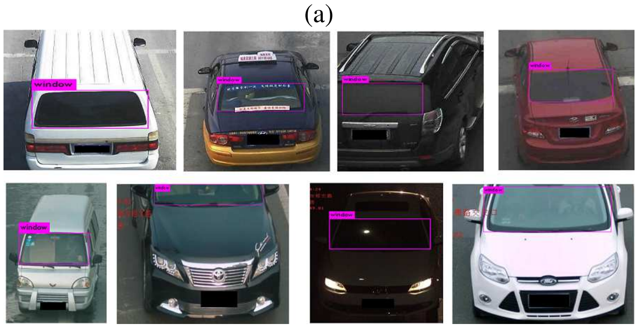

(b)

Figure 4. Visualization of the part detection module. (a) shows the detection result of the light in different viewpoint, notice that in some image light is invisible and can not be detect. (b) shows the detection result of the vehicle window.

modified as

$$\arg\min_{\boldsymbol{\theta}} \mathbb{E}\left(\phi(\boldsymbol{x};\boldsymbol{\theta})^\top \boldsymbol{w}_g, \boldsymbol{y}\right) + \sum_{p\in\mathbb{P}} \lambda_p \mathbb{E}\left(\left(\phi(\boldsymbol{x};\boldsymbol{\theta}) \circledast M_p\right)^\top \boldsymbol{w}_l, \boldsymbol{y}\right), \quad (3)$$

where $\boldsymbol{y} \approx \boldsymbol{y}_p$, now we can use vehicle identification label to optimize our model.

3.3. Training Scheme

Both of our part localization module and part feature extraction and aggregation module can be trained end to end using backpropagation. We adopt the successful YOLO network [19] as our backbone of $LocalNet$. In training steps, first we train the part detection module and extract all the part locations of the training images. Part information of the test images was not extracted since we don't use local feature branch at test stage. For VehicleID and VeRi-776, we adopt the transfer learning scheme and use the ImageNet pretrained weights for backbone network $GlobalNet$(ResNet-50). Then we use the optimization function defined in Eq. (3) with a initial learning rate $lr = 0.01$ with exponential learning rate schedule to finetune the whole feature extraction module, including global and local branch.

4. Experiment

4.1. Datasets and Evaluation Metric

We evaluate our proposed model on two public large-scale vehicle re-identification datasets, VehicleID and VeRi-776.

VeRi-776 is a benchmark dataset for vehicle re-id task. It contains about 50,000 images of 776 vehicles labeled with rich attributes, e.g. types, colors, brands, license plate annotation and spatiotemporal relation annotation. Each vehicle was captured by various cameras with different view points. The short coming of this dataset is that the number of identities is relatively small, in test stage it is very easy to distinguish each vehicle just based on model information. We use the official dataset settings and adopt mAP, HIT-1 and HIT-5 to evaluate our proposed model.

VehicleID is another benchmark with larger data volume. VehicleID is captured by multiple non-overlapping cameras and there are 221,763 images of 26,267 vehicles in total. Each image is either captured from the front view or back view. In VehicleID, only 250 vehicle models are included, which means many different identities share same vehicle model, near-duplicate problem appears. We use mAP to evaluate our method on three subset(i.e. small, medium and large) of the testset.

There are no bounding box annotations of the vehicle parts in both the VehicleID and VeRi-776 dataset. Therefore, we randomly select 500 vehicle images from the VehicleID dataset and label three vehicle parts with bounding boxes (window, light and brand), and these images are used to train the YOLO model. The trained model shows impressive detection results on both VehicleID and VeRi-776 dataset, implying a good generalization ability. The annotation process is also quite efficient and costs only 4 hours of one person in annotating all the 500 images.

The mean average precision (mAP) and cumulative match curve (CMC) are adopted in our experiments. For VeRi-776, the image-to-track metric HIT@1 and HIT@5 is also reported. The CMC curve shows the probability that the image of the probe identity appears in different-sized retrieved list. CMC can be calculated as

$$CMC@k = \frac{\sum_{i=1}^{N} m(q_i, k)}{N}, \quad (4)$$

where N is the number of queries and $m(q_i, k)$ equals to 1 if q_i appears in the top-k of the rank list. The number of ground truth image of a probe should be exactly 1 in order to use the cumulative match curve. The precision measures the accurate of the prediction, the average precision for each query q can be calculated as

$$AP(q) = \sum_{k=1}^{N} P(k)\Delta r(k), \quad (5)$$

where $P(k)$ is the precision at a cutoff of k images, N is the total number of images in the gallery, and $\Delta r(k)$is the change in recall that happened between cutoff $k-1$ and cutoff k. The mean average precision for all query images is determined by

$$mAP = \frac{\sum_{q=1}^{N} AP(q)}{Q}, \tag{6}$$

where Q is the total number of queries.

4.2. Experiment Setup

We use ResNet-50 as the backbone network for feature extraction. We apply average global pooling[11] on the global feature map followed with a 1×1 convolutional layer to extract the final 256-d global feature vector. Euclidean distance (L2) was adopted to compute similarity score between query and gallery images at both training and testing stage. It is worth mentioning that we only use global branch at test stage because during the experiment we found that fusing global and local part features yields similar performance compared to just using global branch, Which mean our model does not need part detection at test stage.

4.3. Comparison with State-of-the-art

The proposed method is compared with state-of-the-art vehicle re-identification methods on two datasets.

VehicleID. For VehicleID dataset, testing data is split into three subsets ordered by their size. For each test dataset split, one image of each vehicle identity is selected and putted into the gallery set. The rest images are all probe queries. In this setting each vehicle identity has many query images but have only one gallery images, so the cumulative match curve (CMC) metric is adopted for evaluation. Table 1 and Table 2 show performance comparisons on VehicleID. Our model outperform all the existing method. OIFE [24] and VAMI [36] exploit the vehicle view information use the view invariant feature to roughly alight the vehicle image. Those view align methods are useful when distinguish different vehicles from difference vehicle model, but they can't address the near-duplicate problem since appearance of same viewpoint of the near-duplicate vehicles are still fairly similar. It need more detail cues than vehicle view informations to distinguish the near-duplicate vehicle.

VeRi-776. The cross-camera search is performed followed the official settings in [14]. At test stage, each image of a vehicle from every camera is selected as probe image and used to search for tracks of the same vehicle in other cameras. That means evaluation for VeRi-776 is conducted in an image-to-track fashion, in which the probe is an image, while the targets are images in the track. The problem is how to define the similarity between a query image and a gallery track. Following the settings in [14], the similarity is defined as maximum similarity between a query image and all images in the track. The image-to-track evaluation results is shown in Table 3. Fact+Plate+STR [14], Siamese+Path [21] and OIFE+ST [24] relies on the spatil-temporal information in Veri-776 Dataset. Fact+Plate+STR [14] uses the additional license plate informations. Other methods only rely on the visual information including ours. Our Part-regularized model outperform all the existing method on mAP metric

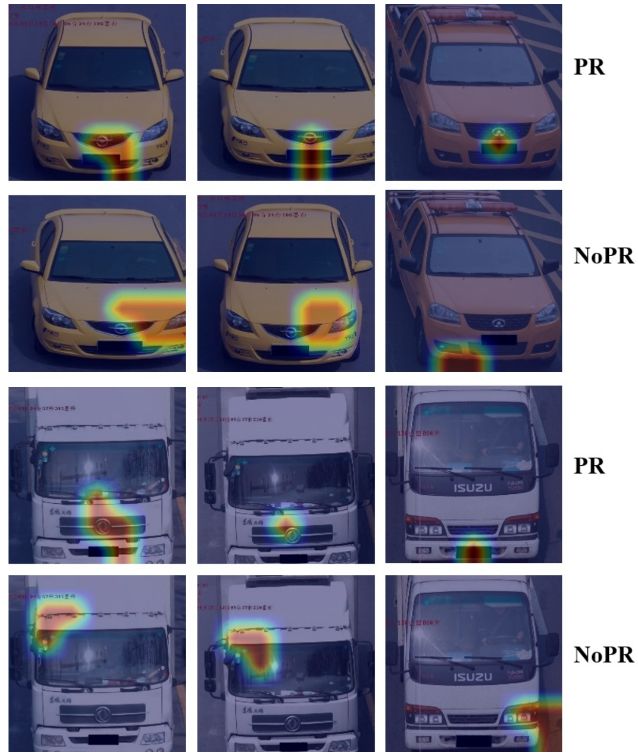

Figure 5. Class activation map (CAM) generated by identification classification model. CAMs with (part-regularized) PR method are show in the first and third rows while NoPR are in the second and forth rows. Activation maps with PR can easily distinguish different cars by the accurate part information for near-duplicated vehicles while NoPR models are usually get confused. It is worth mentioning that the activation map without RP can attend to vehicle light or brand parts originally.

Table 1. Result of CMC@1 in VehicleID Dataset.

Method	Small	Medium	Large
VGG+Triplet Loss [2]	0.404	0.354	0.319
VGG+CCL [12]	0.436	0.370	0.329
Mixed Diff+CCL [12]	0.490	0.428	0.382
OIFE [24]	-	-	0.670
VAMI [36]	0.631	0.529	0.473
Ours	**0.784**	**0.750**	**0.742**

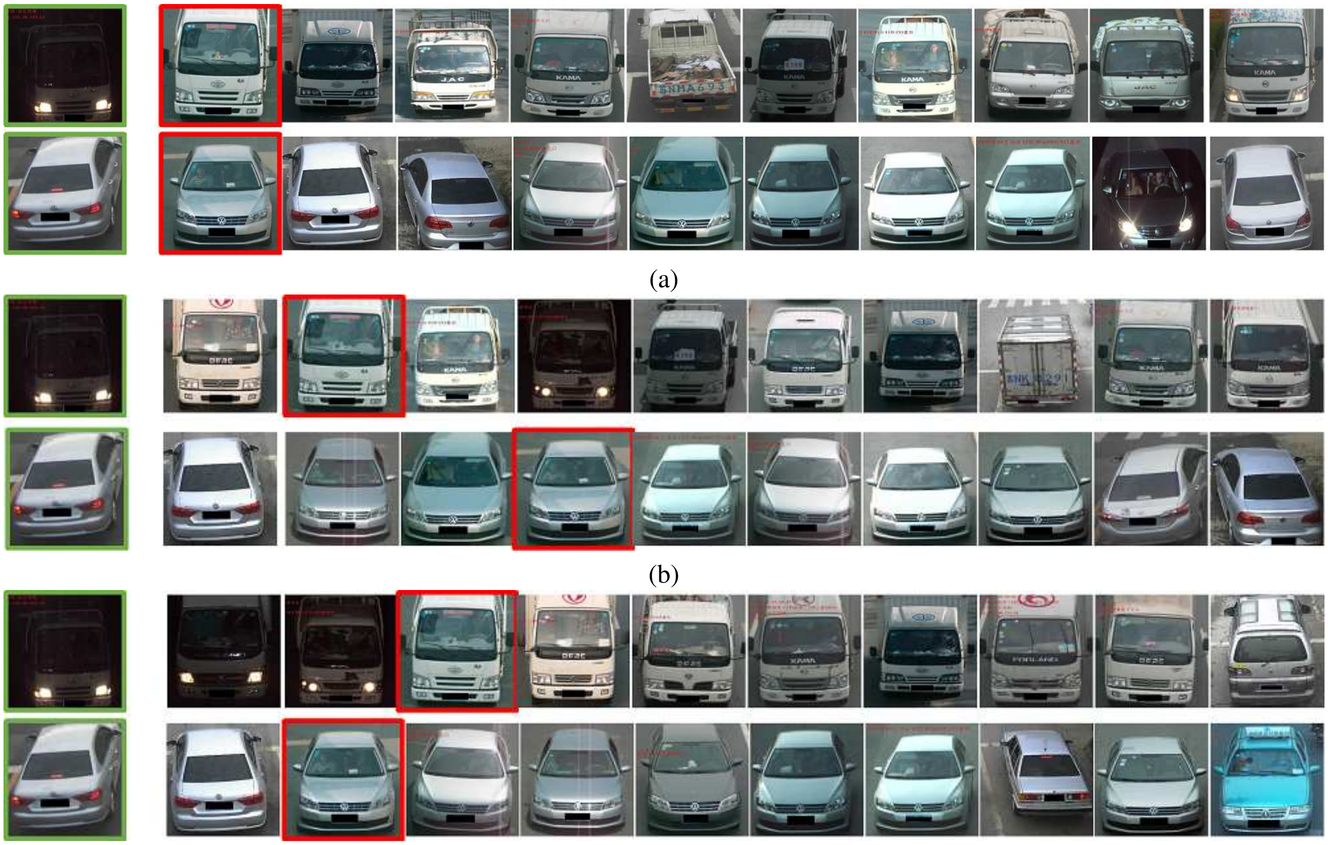

(a)

(b)

(c)

Figure 6. Rank list visualization. The first image with green border in each row is the query image , the rest images are retrieved from the gallery and sorted by similarity score (L2 distance). The ground-truth is marked with red border. (a) rank list result of our full model with all three part branch. The first image in each raw is the query, and the rest ten images are the top ten retrieval results. (b) rank list result after removing the window branch. (c) rank list result after removing the lights and brand branches.

Table 2. Result of CMC@5 in VehicleID Dataset.

Method	Small	Medium	Large
VGG+Triplet Loss [2]	0.617	0.546	0.503
VGG+CCL [12]	0.642	0.571	0.533
Mixed Diff+CCL [12]	0.735	0.668	0.616
OIFE [24]	-	-	0.829
VAMI [36]	0.833	0.751	0.703
Ours	**0.923**	**0.883**	**0.864**

including those who use extra none-visual cues.

4.4. Ablation Study

We conduct ablation study on VehicleID dataset to investigate the effeteness of each part branch in our model. There are three local part branch in our framework, window branch, light branch and brand branch. We remove one branch at a time and retrain the whole network to evaluate the performance. Rank list visualization is also performed as shown in Fig. 6.

Table 3. Results of mAP and HIT@1 HIT@5 in VeRi-776 Dataset.

Method	mAP	HIT@1	HIT@5
BOW-CN [35]	0.122	0.339	0.537
LOMO [9]	0.096	0.253	0.465
GoogLeNet [28]	0.170	0.498	0.712
FACT [13]	0.185	0.510	0.735
Plate-SNN [14]	0.157	0.363	0.466
FACT+Plate-REC [14]	0.186	0.512	0.736
FACT+Plate-SNN [14]	0.259	0.611	0.774
FACT+Plate+STR [14]	0.278	0.614	0.788
Siamese+Path [21]	0.583	0.835	0.900
OIFE [24]	0.480	0.894	-
OIFE+ST [24]	0.514	0.924	-
VAMI [36]	0.501	-	-
Ours	**0.743**	**0.943**	**0.987**

Table 4. Results of Match Rate of ablation experiment.

Method	CMC@1	CMC@5
Global+Light+Brand+Window	0.742	0.864
Global+Light+Brand	0.675	0.830
Global+Light+Window	0.710	0.887
Global+Window+Brand	0.726	0.851
Global+Window	0.707	0.832
Window+Light+Brand	0.687	0.829
Baseline (w/o parts)	0.645	0.800

Table 5. Influences of different resolutions in VehicleID dataset.

VehicleSet	Input size	CMC@1	CMC@5
Small	128×128	0.726	0.886
	256×256	0.784	0.923
Medium	128×128	0.685	0.838
	256×256	0.750	0.883
Large	128×128	0.661	0.819
	256×256	0.742	0.864

Vehicle window. As shown in Table 4, cutting off the vehicle window branch depress the re-id performance by 7 percent. Vehicle window contains the personality feature which is crucial to distinguish difference vehicle identities from same vehicle model. The visualization result confirms this point. As shown in Fig 6, almost all of the top 10 retrieval results are come from the same vehicle model. In this scenario visual cues from vehicle window become extremely important since others vehicle parts are almost the same.

Vehicle brand and light. Removing the vehicle brand or vehicle light branch also depress the performance of our model. Compared to cutting off the vehicle window branch, removing the vehicle light and brand only yields a smaller performance drop. This is because the global feature can learn some of the vehicle light and brand information originally as discussed before in Fig 5. The performance drop shows that putting explicit constrains to the neural network makes the learning process more efficient.

Global branch. We cutting off the global branch and only use three part branch to train the network. During testing three part feature vector is extracted and fusing together to computer the similarity score. The performance drops a lot unsurprisingly. The other part like vehicle body and wheels are useful when distinguish two vehicle identities. The global branch is response to extract those descriminative information.

Influences of resolution. We conduct experiments on different resolutions of input size, as shown in Tab. 5 and 6. For VehicleID dataset, we conduct experiments on three testset with different image resolutions. One intuitive observation is that images with higher resolution performs better

Table 6. Influences of different resolutions in VeRi-776 dataset.

Input size	mAP	HIT@1	HIT@5
128×128	0.653	0.878	0.959
256×256	0.702	0.922	0.979
512×512	0.743	0.943	0.987

but with a higher computation cost. Interestingly, we find that images with size 128×128 exhibit large performance drop especially for CMC@1 indicator, while for CMC@5 and HIT@5, images with low resolution yield feasible results.

5. Conclusions

In this paper, we explore the near-duplicate challenge which causes one of the most remarkable confusions in vehicle re-identification tasks. To enlarge the divergences between nearly identical instances, we proposed a simple but efficient part-regularized approach which enhances the local features in the original Re-ID task. Our model introduces part level constrains to the typical Re-ID framework to enhance the perceptive of subtle discrepancies, which is crucial for the near-duplicate vehicle Re-ID, not being ignored during forward propagation and the detection ROIs on feature maps is the best practice to facilitate the local visual cues. We also conduct qualities and quantities experiments to demonstrate the effectiveness of each branch in our framework.

Acknowledgments

This work was supported in part by the National Basic Research Program of China under Grant 2015CB351806, in part by the National Natural Science Foundation of China under Grant 61672072, Grant 61532003, and Grant 61825101, and in part by Beijing Nova Program under Grant Z181100006218063.

References

[1] Y. Bai, Y. Lou, F. Gao, S. Wang, Y. Wu, and L. Duan. Group sensitive triplet embedding for vehicle re-identification. *TMM*, 2018.

[2] S. Ding, L. Lin, G. Wang, and H. Chao. Deep feature learning with relative distance comparison for person re-identification. *PR*, 48(10), 2015.

[3] J. Fu, H. Zheng, and T. Mei. Look closer to see better: Recurrent attention convolutional neural network for fine-grained image recognition. In *CVPR*, volume 2, 2017.

[4] K. He, X. Zhang, S. Ren, and J. Sun. Deep residual learning for image recognition. In *CVPR*, 2016.

[5] S. Huang, Z. Xu, D. Tao, and Y. Zhang. Part-stacked cnn for fine-grained visual categorization. In *CVPR*, 2016.

[6] M. M. Kalayeh, E. Basaran, M. Gökmen, M. E. Kamasak, and M. Shah. Human semantic parsing for person re-identification. In *CVPR*, 2018.

[7] D. Li, X. Chen, Z. Zhang, and K. Huang. Learning deep context-aware features over body and latent parts for person re-identification. In *CVPR*, 2017.

[8] D. Li, X. Chen, Z. Zhang, and K. Huang. Learning deep context-aware features over body and latent parts for person re-identification. In *CVPR*, 2017.

[9] S. Liao, Y. Hu, X. Zhu, and S. Z. Li. Person re-identification by local maximal occurrence representation and metric learning. In *CVPR*, 2015.

[10] D. Lin, X. Shen, C. Lu, and J. Jia. Deep lac: Deep localization, alignment and classification for fine-grained recognition. In *CVPR*, 2015.

[11] M. Lin, Q. Chen, and S. Yan. Network in network. *arXiv preprint arXiv:1312.4400*, 2013.

[12] H. Liu, Y. Tian, Y. Yang, L. Pang, and T. Huang. Deep relative distance learning: Tell the difference between similar vehicles. In *CVPR*, 2016.

[13] X. Liu, W. Liu, H. Ma, and H. Fu. Large-scale vehicle re-identification in urban surveillance videos. In *Multimedia and Expo (ICME), 2016 IEEE International Conference on*. IEEE, 2016.

[14] X. Liu, W. Liu, T. Mei, and H. Ma. A deep learning-based approach to progressive vehicle re-identification for urban surveillance. In *ECCV*. Springer, 2016.

[15] Y. Lou, Y. Bai, J. Liu, S. Wang, and L.-Y. Duan. Embedding adversarial learning for vehicle re-identification. *IEEE Transactions on Image Processing*, 2019.

[16] P. Luo, X. Wang, and X. Tang. Hierarchical face parsing via deep learning. In *CVPR*. IEEE, 2012.

[17] J.-J. Lv, X. Shao, J. Xing, C. Cheng, X. Zhou, et al. A deep regression architecture with two-stage re-initialization for high performance facial landmark detection. In *CVPR*, volume 1, 2017.

[18] O. M. Parkhi, A. Vedaldi, C. Jawahar, and A. Zisserman. The truth about cats and dogs. In *ICCV*. IEEE, 2011.

[19] J. Redmon, S. Divvala, R. Girshick, and A. Farhadi. You only look once: Unified, real-time object detection. In *Proceedings of the IEEE conference on computer vision and pattern recognition*, pages 779–788, 2016.

[20] F. Schroff, D. Kalenichenko, and J. Philbin. Facenet: A unified embedding for face recognition and clustering. In *CVPR*, 2015.

[21] Y. Shen, T. Xiao, H. Li, S. Yi, and X. Wang. Learning deep neural networks for vehicle re-id with visual-spatio-temporal path proposals. In *ICCV*. IEEE, 2017.

[22] C. Su, J. Li, S. Zhang, J. Xing, W. Gao, and Q. Tian. Pose-driven deep convolutional model for person re-identification. In *ICCV*. IEEE, 2017.

[23] Y. Sun, X. Wang, and X. Tang. Deep convolutional network cascade for facial point detection. In *CVPR*, 2013.

[24] Z. Wang, L. Tang, X. Liu, Z. Yao, S. Yi, J. Shao, J. Yan, S. Wang, H. Li, and X. Wang. Orientation invariant feature embedding and spatial temporal regularization for vehicle re-identification. In *CVPR*, 2017.

[25] K. Q. Weinberger and L. K. Saul. Distance metric learning for large margin nearest neighbor classification. *Journal of Machine Learning Research*, 10(Feb), 2009.

[26] T. Xiao, H. Li, W. Ouyang, and X. Wang. Learning deep feature representations with domain guided dropout for person re-identification. In *CVPR*, 2016.

[27] K. Yan, Y. Tian, Y. Wang, W. Zeng, and T. Huang. Exploiting multi-grain ranking constraints for precisely searching visually-similar vehicles. In *ICCV*, 2017.

[28] L. Yang, P. Luo, C. Change Loy, and X. Tang. A large-scale car dataset for fine-grained categorization and verification. In *CVPR*, 2015.

[29] H. Zhang, T. Xu, M. Elhoseiny, X. Huang, S. Zhang, A. Elgammal, and D. Metaxas. Spda-cnn: Unifying semantic part detection and abstraction for fine-grained recognition. In *CVPR*, 2016.

[30] N. Zhang, J. Donahue, R. Girshick, and T. Darrell. Part-based r-cnns for fine-grained category detection. In *ECCV*. Springer, 2014.

[31] X. Zhang, H. Luo, X. Fan, W. Xiang, Y. Sun, Q. Xiao, W. Jiang, C. Zhang, and J. Sun. Alignedreid: Surpassing human-level performance in person re-identification. *arXiv preprint arXiv:1711.08184*, 2017.

[32] X. Zhang, H. Xiong, W. Zhou, W. Lin, and Q. Tian. Picking deep filter responses for fine-grained image recognition. In *CVPR*, 2016.

[33] Z. Zhang, P. Luo, C. C. Loy, and X. Tang. Facial landmark detection by deep multi-task learning. In *ECCV*. Springer, 2014.

[34] H. Zhao, M. Tian, S. Sun, J. Shao, J. Yan, S. Yi, X. Wang, and X. Tang. Spindle net: Person re-identification with human body region guided feature decomposition and fusion. In *CVPR*, 2017.

[35] L. Zheng, L. Shen, L. Tian, S. Wang, J. Wang, and Q. Tian. Scalable person re-identification: A benchmark. In *CVPR*, 2015.

[36] Y. Zhou and L. Shao. Aware attentive multi-view inference for vehicle re-identification. In *CVPR*, 2018.

[37] S. Zhu, C. Li, C. Change Loy, and X. Tang. Face alignment by coarse-to-fine shape searching. In *CVPR*, 2015.